Immunohistochemical quantification of serotonin and serotonin transporters in the lumbar region of the mouse spinal cord after spinal cord injury

Honors Thesis
Presented to the College of Arts and Sciences
Cornell University
in Partial Fulfillment of the Requirements for the
Biological Sciences Honors Program

by
Diana Nayoun Hong
May 2013
Dr. Ronald Harris-Warrick

Immunohistochemical quantification of serotonin and serotonin transporters in the lumbar region of the mouse spinal cord after spinal cord injury

Diana N. Hong
Department of Neurobiology and Behavior, Cornell University

Central pattern generators (CPGs) are important neuronal networks that are made up of interneurons that organize rhythmic motor output such as respiration, mastication, and locomotion. Locomotor CPGs are located in the spinal cord of all vertebrates. Interneurons have been shown to be a necessary part of regulating the coordination of the left and right flexor and extensor muscles that generate the normal walking movement. The V2a interneurons, in particular, play an important role in maintaining a left-right alternating hindlimb pattern at high speeds. Two key players of the CPGs are serotonin (5-HT) and serotonin transporters (SERT). 5-HT plays an important role in enabling the network to generate the locomotor rhythm in rodents, while SERT is responsible for high affinity uptake of 5-HT to terminate its activity in the synaptic cleft. Using double immunohistochemical methods, I determined that not only are 5-HT and SERT co-localized in 5-HT terminals, but also 5-HT and SERT–labeled terminals are located on V2a interneurons. Using Sholl analysis, I determined that SERT and 5-HT show similar co-localization patterns on the V2a interneurons. Although spinal cord injury (SCI) typically does not inflict physical damage to the cells that make up the hindlimb CPG, it results in a loss of motor function by removing descending input from the brain. This in turn can induce changes in CPG cellular activity and transmitter sensitivity. Thus, I sought to observe how SCI affects expression levels of 5-HT and SERT. After SCI, a loss of motor function occurs due to the changes in cellular activity and sensitivity in the CPG. Using single immunohistochemical methods, I determined that both 5-HT and SERT decrease significantly in area and intensity after SCI.

Introduction

Central pattern generators (CPGs) are important neuronal networks, made up of interneurons, which organize rhythmic motor output such as respiration, mastication, and locomotion (Barlow, 2009; Kiehn, 2006). The CPG for locomotion is located (Zhong et al., 2010) in the spinal cord of all vertebrates (Kiehn, 2006). Interneurons have been shown to regulate the coordination of the left and right flexor and extensor muscles (Zhong et al., 2010). Some of these interneurons can be visually labeled and identified using fluorescent marker proteins based on their patterns of transcription factor expression (Guertin, 2005; Kiehn, 2011). Identified by the expression of the transcription factor Chx10, the V2a class of interneurons is not essential for locomotor-like rhythm generation but has been shown to play an important role in maintaining left-right alteration at high locomotor cycle frequencies (Zhong et al., 2010). These glutamatergic, ipsilaterally projecting neurons are rhythmically active during fictive locomotion (Zhong et al., 2010).

Two key molecular players in the CPG are serotonin and serotonin transporters. Previous studies have shown that serotonin, or 5-hydroxytryptamine (5-HT), has an important role in the generation of the locomotor rhythm in rodents (Schmidt and Jordan, 2000; Zhong et al., 2010). Descending serotonergic fibers originating from the medullary Raphe nuclei provide the serotonergic input to the lumbar spinal cord region (Schmidt and Jordan, 2000). During the time of locomotion, serotonin release in the lumbar spinal cord has been observed in rodents, which can help to prepare the CPG network to generate fictive locomotion (Schmidt and Jordan, 2000). Fictive locomotor-like activity can be induced when the ventral half of the spinal cord is infused with 5-HT and NMDA (Zhong et al., 2010). 5-HT transmission is terminated by serotonin

transporters (SERT), a 12 transmembrane sodium and calcium-dependent transporter. SERT has been found within nanometers of the synapse as well as at greater distances, and it has been shown that the 5-HT molecules that are not taken up by the perisynaptic SERT are taken up into the same or neighboring cells through axonal SERT or nearby glial cells (Zhou et al., 1998). Since SERT is responsible for the high affinity uptake of 5-HT, and thus the removal of the 5-HT from the synaptic cleft, the activity of SERT determines the time course of 5-HT in the postsynaptic cell (Zhou et al., 1998).

Spinal cord injury (SCI) results in the immediate and irreversible loss of sensory perception and motor function below the injury site (Guertin, 2005). Although SCI typically does not inflict physical damage to the cells that make up the hindlimb CPG, it results in a loss of motor function by removing descending input from the brain, including the activating reticulospinal glutamate pathway and the Raphe serotonergic pathway (Fourad et al., 2010; Hayashi et al., 2010). This in turn can induce changes in CPG cellular activity and transmitter sensitivity. Following SCI, motoneurons below the lesion become hyperexcitable due to an increased expression of slow inward currents, and also demonstrate 5-HT denervation supersensitivity (Bennett and Siu, 2001; Kong et al., 2011). Furthermore, a downregulation of SERT has been shown in rats after SCI (Kong et al., 2011). This may result from the localization of SERT in the spinal cord on the terminals of the descending serotonergic fibers (Schmidt and Jordan, 2000).

The goal of my project was to determine the changes in 5-HT and SERT expression after SCI using immunohistochemical methods in the regions of the spinal cord where the Chx-10 interneurons are located. First, by performing double immunohistochemistry, the approximate locations of SERT and 5-HT relative to each other and relative to the V2a interneurons were

determined. The results from these co-localization studies showed that not only do SERT and 5-HT co-localize, but SERT and 5-HT–labeled processes are located on V2a neurons in a similar manner, suggesting similar patterns of synaptic contact. Then single immunohistochemistry was performed on both SCI and intact mice to address the changes in expression levels, as measured by area and intensity, of 5-HT and SERT. These experiments showed that both the area and intensity of 5-HT and SERT significantly decreased after SCI.

Materials and Methods

Transgenic mice. Chx10::eCFP mice, which were provided by Drs. Steven Crone and Kamal Sharma at the University of Chicago, were used for the following experiments. The mice were maintained and bred at Cornell following accepted IACUC policies.

SCI surgery. 3- to 4-week-old mice were used for SCI surgery; the surgery was performed by a technician in our laboratory. Once under anesthesia, the mouse's dorsal skin was shaved and sterilized in preparation for an incision to expose the part of the vertebral column dorsally above the thoracic region of the spinal cord. A gap was made between the T8 and T9 vertebrae, and a complete transverse cut to the spinal cord was made. The incision was closed with tissue glue. Post-operative care, including drug administration and bladder expression, was administered. Littermates were used as controls. Mice were maintained by the technician for 4 to 5 weeks until they were used.

Perfusion. SCI mice and their age-matched control intact mice were anesthetized with 0.03 mg/g of ketamine/xylazine IP 4-5 weeks after surgery. Once deeply anesthetized, the mice were prepared for perfusion. In the fume hood, with the mouse's ventral side up, an incision was made to expose the peritoneal cavity. The left and right ribcages were cut laterally and the diaphragm was then cut horizontally to expose the heart. A cut was made in the right atrium to drain the blood, and a 25 gauge needle attached to a perfusion pump was inserted into the left ventricle. Once the liver blanched, perfusion buffer was perfused through the mice for 3 minutes, and 4% PFA in 0.1M phosphate buffer was then perfused for 20 minutes. A laminectomy was performed in order to remove the spinal cord. The isolated spinal cord was post-fixed in 4% paraformaldehyde at 4° C for 90 minutes. The cord was then dehydrated in 30% sucrose at 4° C 16 hours.

Cryostat sectioning. From the post-fixed and dehydrated spinal cords, a 1 mm segment of the upper lumbar spinal cord was cut. Two spinal cords were positioned side by side on the chuck and cut into 15 micron transverse slices using a cryostat. For the double immunohistochemistry experiments, two intact cords were placed side by side; for the single immunohistochemistry experiments, a SCI and control, intact cords were placed side by side. Slices were plated onto microscope slides (25x8x1mm, Fisherbrand Superfrost), so that 8 slices of both SCI and intact spinal cords were arranged in pairs evenly on the microscope slides (Figure 1). These slides were then stored at -20° C until they were used for IHC.

Fig. 1. Arrangement of spinal cord pairs on one microscope slide. SCI- and intact- spinal cords were sectioned together and placed at one of eight positions.

*Figure 1 was reproduced with permission from Scaperotti, 2012.

Single immunohistochemistry. A blocking pap-pen was used to enclose each pair of spinal cord slices on each of the microscope slides. At room temperature, the slides were first washed with 1X phosphate buffered saline (PBS) (1.5M NaCl, 3.8 mM NaH_2PO_4, 16.2mM Na_2HPO_4) for 4 minutes. They were then incubated with 0.2% Triton X-100 for 10 minutes. Afterwards, the slices were washed with 1X PBS three times over 15 minutes. Exogenous peroxidase activity was quenched with peroxidase quenching buffer for 60 minutes at room temperature. 1% blocking reagent (Invitrogen Tyramide Signal Amplification Kit) was applied for 60 minutes, also at room temperature, in order to bind nonspecific ligands and prevent inappropriate binding of the primary antibody. Primary antibodies, raised in rabbits, were diluted (SERT 1:1000, ImmunoStar; 5-HT 1:5000, Sigma) and applied to spinal cord slices for 16 hours at 4° C. Additionally, one of the positions on the microscope slide was incubated in 1% blocking reagent alone as a no-primary control. Another position was designated as the preabsorption control. The SERT peptide used as the epitope to make the antibody (Immunostar) was preabsorbed with the anti-SERT antibody (1:1000) for 18 to 21 hours. This mixture was then applied to the designated position on the microscope slide. Slides were rinsed in 4°C 1X PBS three times over 15 minutes. They were then incubated in anti-rabbit secondary antibody conjugated to horseradish peroxidase (Invitrogen SA kit) diluted 1:100 in 1% blocking reagent for 45 minutes at room temperature in order to amplify and detect the primary antibodies. Slides were rinsed in 4°C 1X PBS three times over 15 minutes and incubated in Alexa Fluor 647 tyramide, diluted 1:100 in amplification buffer/0.0015% H2O2 for 16 minutes. The tyramide immunofluorescence procedure was used because it allows for signal amplification and is thus useful when there are few target antigens or

when there is a high amount of nonspecific background signals. During the tyramide amplification procedure, the secondary antibody is conjugated to HRP, and this then reacts with an inactive tyramide derivative to produce a fluorescent tag on the secondary antibody. The signal at each antigen is amplified because the HRP-derivative reaction occurs repeatedly at each secondary antibody. After the 16 minutes of incubation, slides were rinsed in 4°C 1X PBS three times over 15 minutes and mounted with Fluor-Gel with Tris buffer (Electron Microscopy Sciences) and coverslipped (22x50 mm, Electron Microscopy Sciences).

Double Immunohistochemistry. Two primary antibodies were used together, raised in different animals (goat polyclonal to GFP 1:250, Abcam; Rabbit anti-SERT 1:250, Immunostar; Rabbit anti-5-HT 1:1000, Sigma; Goat anti-5-HT 1:1000, Immunostar), and were then reacted with different second antibodies. The rabbit anti-SERT and rabbit anti-5-HT, were incubated in anti-rabbit secondary antibody conjugated to horseradish peroxidase. For the goat polyclonal to GFP, a secondary antibody, donkey polyclonal to goat DyLight 488, was used (1:200 or 1:400).

Microscopy. A LeicaTCS SP2 confocal microscope was used for imaging. For single immunohistochemistry, a 20x objective lens was used to view tissue, and regions of the medial lamina VIII of every spinal cord slice were imaged with 8X zoom for analysis using the 633 nm laser line. Within each experiment, SCI and intact slices of the same pap-circles were imaged using the same microscope gain and offset settings. For double immunohistochemistry, a 63x objective lens was used, with a 4X zoom while simultaneously using the 633nm and 488 nm lasers. For double labeling of SERT and 5-HT, medial lamina VIII of every spinal cord slice was imaged. For double labeling of V2a interneurons (GFP) and 5-HT or SERT, every detectable

V2a interneuron was imaged. No-primary and preabsorption-control positions were imaged with the highest gain-value for each primary antibody using the same microscope settings as for non-control positions. Z-series projections of the 15 μm tissue were made in 1μm step sizes.

Single immunohistochemistry analysis. ImageJ software (v.1.44p; NIH) was used to assemble the Z-series projections into a single image of a max-projection. These images were deconvolved using an ImageJ plug-in to remove any noise from the confocal microscope. Using MatLab, the average pixel intensity in the deconvolved no-primary antibody control images were subtracted from the deconvolved max projections. Each image was converted into a binary image in order to determine the number of pixels above an automated threshold, which were used to determine the percent of pixels above threshold in the paired SCI images. The mean intensity of these pixels was also recorded and compared. Raw data were compared between slices of the same group on a slide while ratios were used for between-experiment comparisons.

Double immunohistochemistry analysis. For double immunohistochemistry mapping of SERT and 5-HT, ImageJ software was used to split the channel images and deconvolve each optical slice for the green (488 nm; 5-HT) and far red (633 nm; SERT) channels. Using MatLab, the average pixel intensity in the deconvolved no-primary antibody control images were subtracted from the deconvolved optical slice images. Then, for each optical slice, the Manders' coefficient plugin was used to determine the percentage of pixels in one channel that co-localize with a signal from the second channel. M1 refers to the percentage of SERT pixels co-localizing with the signal from the 5-HT channel, and M2 refers to the percentage of 5-HT pixels co-localizing with signals from the SERT channel. Therefore, with a greater signal from the 5-HT, the ratio of

5-HT pixels co-localizing with signals from the SERT channel to the total number of 5-HT pixels decreases, and M2 thus decreases (Manders EMM et al., 1993). For double immunohistochemistry labeling for V2a interneurons and SERT and for V2a interneurons and 5-HT, Fiji, an image processing package that is a distribution of ImageJ, was used in order to perform Sholl analysis, a quantification method that counts the number of path intersections for concentric circles of gradually increasing radii that are centered at the cell body (Langhammer et al., 2010). Radius sizes of increasing multiples of 8.206 pixels, or 1 micrometer, were used. In order to ensure that processes of only one V2a interneuron was being analyzed at a time, and any images that showed more than one V2a interneuron cell body was not used for analysis; the V2a interneurons are sparse in the spinal cord, so it is unlikely that processes from a different V2a interneurons are found in the image. The Simple Neurite Tracer plugin was used to highlight the areas of co-localization in the composite image stacks. Once the paths were traced and the V2a interneuron cell was designated as the central point, a Sholl analysis was performed to determine at what distance from the V2a interneuron cell the SERT or 5-HT was co-localizing in highest frequency. A graph was created that allowed for a visualization of how the number of intersections with concentric circles varied with the distance from the central point. The Sholl analysis data obtained from individual V2a interneurons were then compiled and averaged.

Statistical analysis. Statistics were performed using JMP (JMP software; SAS) and Graph Pad Prism (GraphPad Software). For comparison of multiple treatments of Z-series projections 1-way ANOVA was applied. Additionally, single and double immunohistochemistry data were analyzed using the multilevel model (also known as mixed effect model). With this model, for the single immunohistochemistry, the intensity data and area data were response variables, while

the mouse pair and mouse within each pair were set as the random effect, and the type of mouse (SCI or intact mouse) was set as the fixed effect. For the double immunohistochemistry with double labeling for V2a interneurons and 5-HT and with double labeling for V2a interneurons and SERT, the difference between the two Manders' coefficients and was the response variable, the mouse and analyzed optical slice were set as the random effect. A significance level of 0.05 was accepted for all tests.

*Some of the methods listed under the headings of *Transgenic Mice*, *SCI surgery*, *Perfusion*, *Cryostat sectioning*, *Single immunohistochemistry*, *Microscopy*, *Single immunohistochemistry analysis*, and *Statistical analysis* were taken from Husch et al. (2012).

Results

Co-localization of serotonin transporters (SERT) and serotonin (5-HT)

In order to determine where the serotonin transporters (SERT) are located in relation to serotonin (5-HT) and if SERT are indeed located entirely within 5-HT terminals, co-localization analysis of the double immunohistochemical labeling of SERT and 5-HT was performed using Manders' coefficient. With SERT immunostaining being imaged using the far red channel (633 nm) and 5-HT immunostaining being imaged using the green channel (488 nm), red pixels denote the amount of SERT staining and green pixels denote the amount of 5-HT staining (Figure 2). Empty black areas, as seen in Figures 2A and C, are artifacts from the cryostat procedure and are not indicative of staining results.

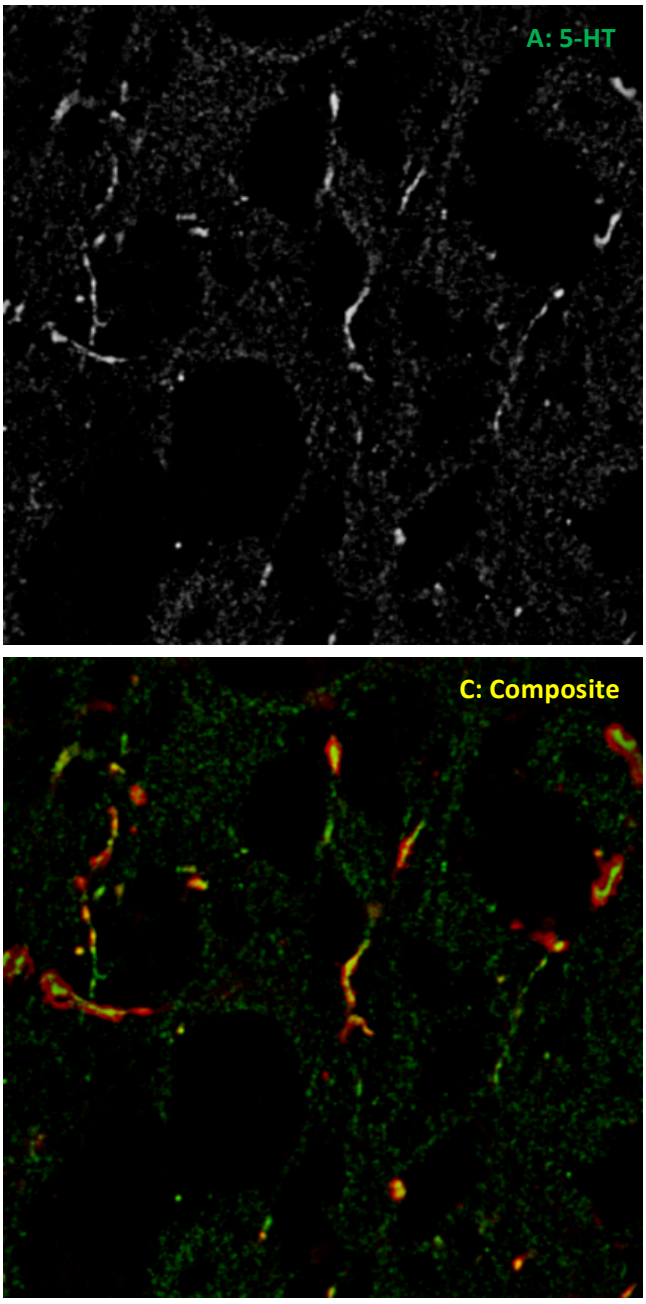

Figure 2. Co-localization analysis of the double immunohistochemical labeling of serotonin (5-HT), in green, and serotonin transporters (SERT), in red. **A**.5-HT labeling from green channel. **B**. SERT labeling from red channel. **C**. Composite image of A and B, showing co-localization in yellow.

M1 is interpreted as the percentage of SERT-labeled pixels co-localizing with the signal from the 5-HT channel, and M2 is interpreted as the percentage of 5-HT pixels co-localizing with signals from the SERT channel. For each optical slice that was analyzed, M2 was less than M1, and the difference between the two coefficients was significant ($p<0.05$, $n=5$). The average M2

coefficient was 0.79, meaning approximately 79% of the imaged SERT co-localized with the imaged 5-HT. Since previous studies showed that virtually all the SERT is located in 5-HT terminals, this M2 coefficient is lower than expected. However, this low percentage of SERT co-localization in 5-HT processes is a conservative estimate and may represent more of an artifact of the analysis than a true demonstration of SERT co-localization. From visual inspection, an almost complete overlap of SERT with 5-HT processes is observed, suggesting that SERT is indeed primarily expressed in 5-HT processes. Furthermore, Manders' coefficients are sensitive to background signals, and pixel slippage can occur while obtaining multiple Z-series. Both of these factors could contribute to the lower than expected M2 value. The average M1 coefficient was 0.54, meaning approximately 54% of the imaged 5-HT co-localized with the imaged SERT. The fact that the M1 coefficient is less than the M2 coefficient illustrates that there is more 5-HT staining alone and not co-localizing with SERT. This is expected since SERT is selectively localized at pre-synaptic terminals of the 5-HT axons (Zhou et al., 1998).

5-HT and SERT show similar co-localization patterns on V2a interneurons

It has previously been shown that the loss of serotonin contributes to a significant increase in 5-HT sensitivity in V2a interneurons (Husch et al., 2012), but it was not yet proven whether V2a interneurons were directly innervated by descending serotonergic fibers. Thus, I sought to determine whether V2a interneurons might receive direct synaptic input from descending 5-HT axons. Double immunohistochemistry labeling for V2a interneurons (using an antibody against CFP in Chx10-CFP mice) and SERT, and for V2a interneurons and 5-HT, were performed in order to determine the existence and distribution of serotonin processes and terminals on the V2a interneurons, suggesting synaptic contact. Yellow pixels, denoting the co-localization of 5-HT

(red channel) and a V2a interneuron (green channel) to within a single pixel, were used as possible markers for synaptic contact. Images were taken from the medial lamina VIII region (see Figure 7A). Before Sholl analysis was performed, areas of double labeling were traced using Simple Neurite Tracer plugin (Figure 3).

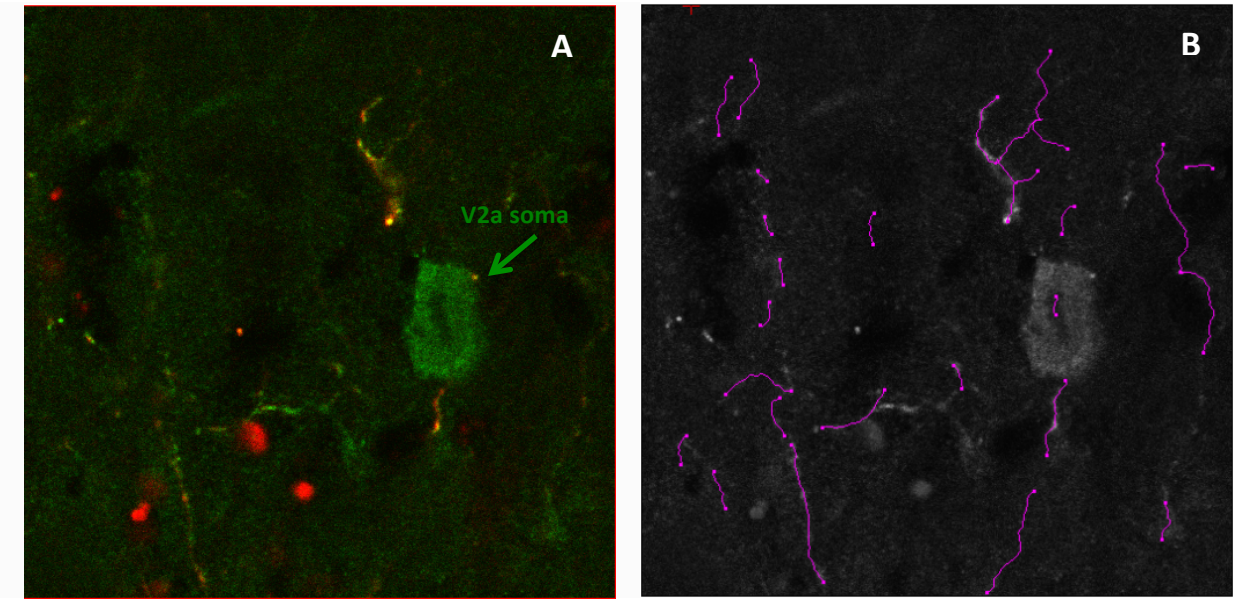

Figure 3. Simple Neurite Tracer application prior to performing Sholl Analysis. **A**. One optical slice showing areas of co-localization of SERT (red) and V2a (green) processes is seen in yellow. **B**. The final traced image of the co-localized areas.

Sholl analysis, a quantification method that counts the number of path intersections for concentric circles of gradually increasing radii that are centered at the cell body (Langhammer et al., 2010), was then performed on the double labeled composite image stacks of V2a interneurons and 5-HT. This analysis determines the distance at which the V2a interneuron and the SERT or 5-HT co-localizes in highest frequency. The number of intersections between the traced co-localized V2a interneuron and 5-HT processes were binned into a set of concentric circles of increasing radius; this Sholl analysis illustrated where on the V2a interneuron the 5-HT terminals were located (n=8 cells, Figure 4A). From the average of these data, it was determined that the peak of the distribution of the crossings occurred about 3 microns from the V2a cell

body (Figure 5). Though synapses cannot be conclusively observed with light microscopes, these co-localizations represent putative 5-HT synapses on the V2a interneurons as one pixel is equivalent to 0.116 um. The same analysis was done for double labeled composite image stacks of V2a interneurons and SERT. Like the 5-HT, the average peak of the distribution of the SERT co-labeling with the V2a interneurons was about 3 microns from the V2a cell body (n=11 cells, Figure 6). Table 1 summarizes the average number of crossings for various radii measurements from the cell body.

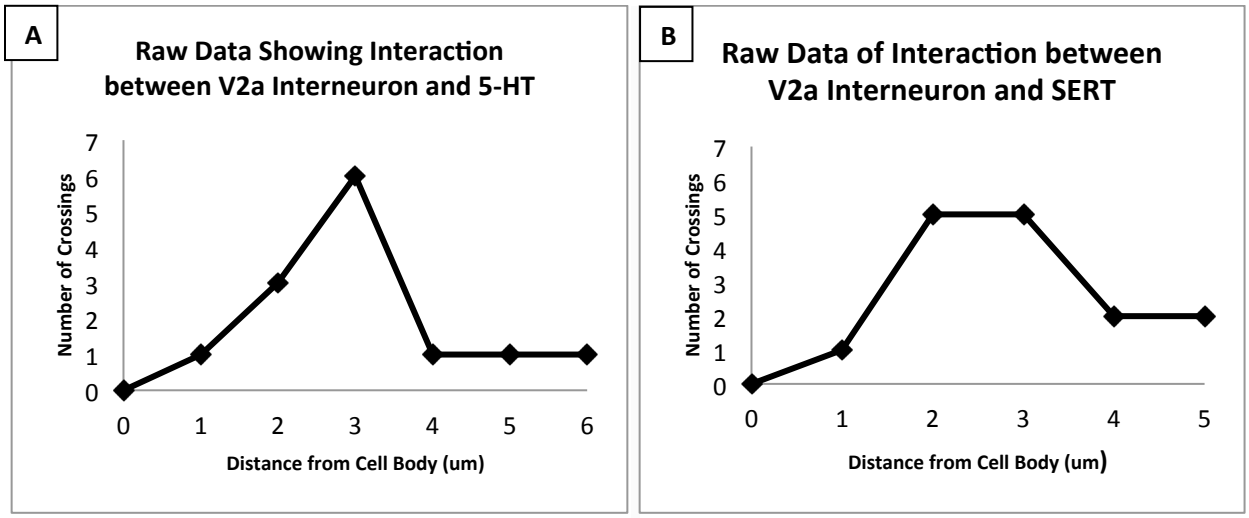

Figure 4. Typical raw data distributions from single V2a Interneurons. **A.** Graph from Sholl Analysis for one V2a interneuron and 5-HT. **B.** Graph from Sholl Analysis for one V2a interneuron and SERT.

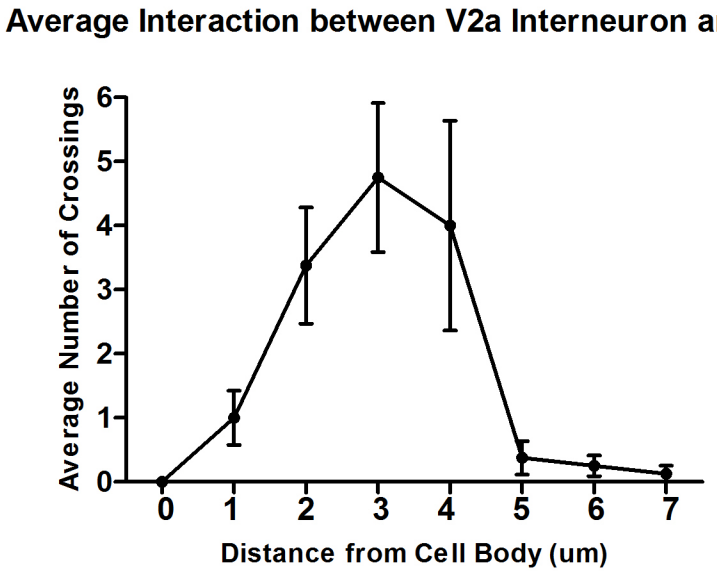

Figure 5. Graph from Sholl analysis showing the average number of intersecting points of 5-HT and V2a processes.

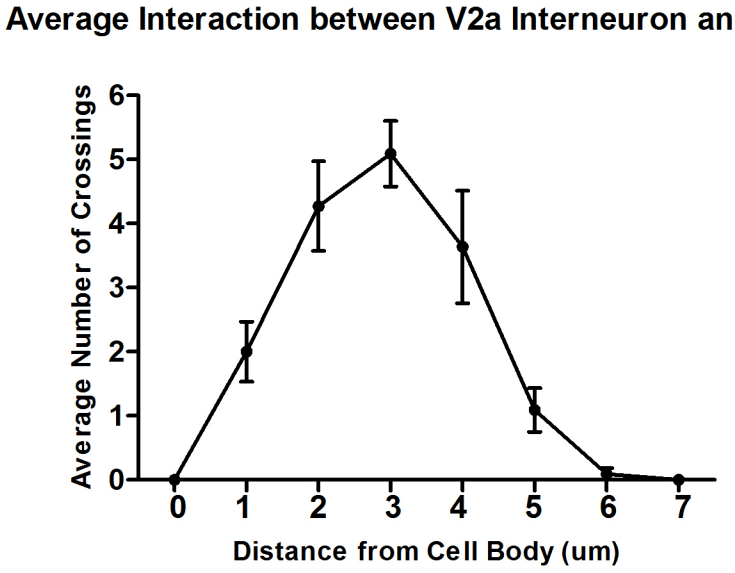

Figure 6. Graph from Sholl analysis showing the average number of intersecting points of SERT and V2a processes.

Table 1. Summary of Sholl Analysis for the Co-localization of V2a Interneurons and 5-HT (n=8 cells) and of V2a Interneurons and SERT (n=11 cells)		
Radius from V2a Interneuron Cell Body (μm)	Average Number of Crossings for 5-HT (mean ± SE)	Average Number of Crossings for SERT (mean ± SE)
0	0 ± 0	0 ± 0
1	1 ± 0.423	2 ± 0.467
2	3.375 ± 0.905	4.273 ± 0.702
3	4.750 ± 1.161	5.091 ± 0.513
4	4 ± 1.637	3.636 ± 0.877
5	0.375 ± 0.264	1.091 ± 0.343
6	0.250 ± 0.164	0.091 ± 0.091
7	0.125 ± 0.125	0 ± 0

Reduction in 5-HT and SERT after SCI

Although my previously described co-localization experiments seem to give evidence that SERT is located in 5-HT terminals, it was not determined whether all the SERT was located there. It is possible that some SERT is in glial or other non-5-HT cells. I wanted to determine if any SERT would be left after SCI, which should eliminate the 5-HT terminals, and if any SERT would remain in glial or other non-5-HT terminals. In order to determine how SCI changes expression levels of 5-HT and SERT, single immunohistochemical analyses of 5-HT and SERT in the medial lamina VIII region of matched pairs of intact and SCI mice were performed by myself and two other researchers in our lab (Figure 7A). While the serotonin immunofluorescence labeling was observed as fibrous staining in the axons of the descending raphe neurons in the control animals (Figure 7B; Carlsson et al., 1964), no fibrous staining was detected after SCI (Figure 7C; Carlsson et al., 1963). Both the serotonergic area, as measured by the percentage of pixels expressing 5-HT immunoreactivity, as well as the serotonergic fiber intensity, as measured by the subthreshold pixels surround the immunoreactive fibers, were significantly lower in SCI mice compared with intact mice. An 85% reduction in pixel number after SCI ($p<0.05$, matched-

pair test, n=12) and an 84.6% reduction in pixel intensity after SCI ($p<0.05$, matched-pair test, n=12) was observed. This significant decrease in 5-HT expression was expected since the great majority of the serotonin in the spinal cord originates from the raphe neuron terminals, located in the brainstem (Carlsson et al., 1964) and this descending supply is cut by a complete SCI (Hayashi et al., 2010). With the loss of the descending 5-HT terminals after SCI, the majority of the SERT, which is found on 5-HT terminals (See Figure 2 above) and removes 5-HT from the synaptic cleft (Zhou et al., 1998), would also be expected to decrease. As expected, fibrous SERT immunostaining was significantly reduced after SCI. While fibrous SERT immunostaining was readily observed in the ventromedial cord of intact mice, less fibrous staining was detected after SCI (Figure 7G, Hayashi et al., 2010). As with the 5-HT immunostaining, both the SERT area and the SERT intensity were significantly lower in SCI mice compared with intact mice. A 51.4% reduction in pixel number after SCI ($p<0.05$, matched-pair test, n=6) and a 49.4% reduction in pixel intensity after SCI ($p<0.05$, matched-pair test, n=6) was observed.

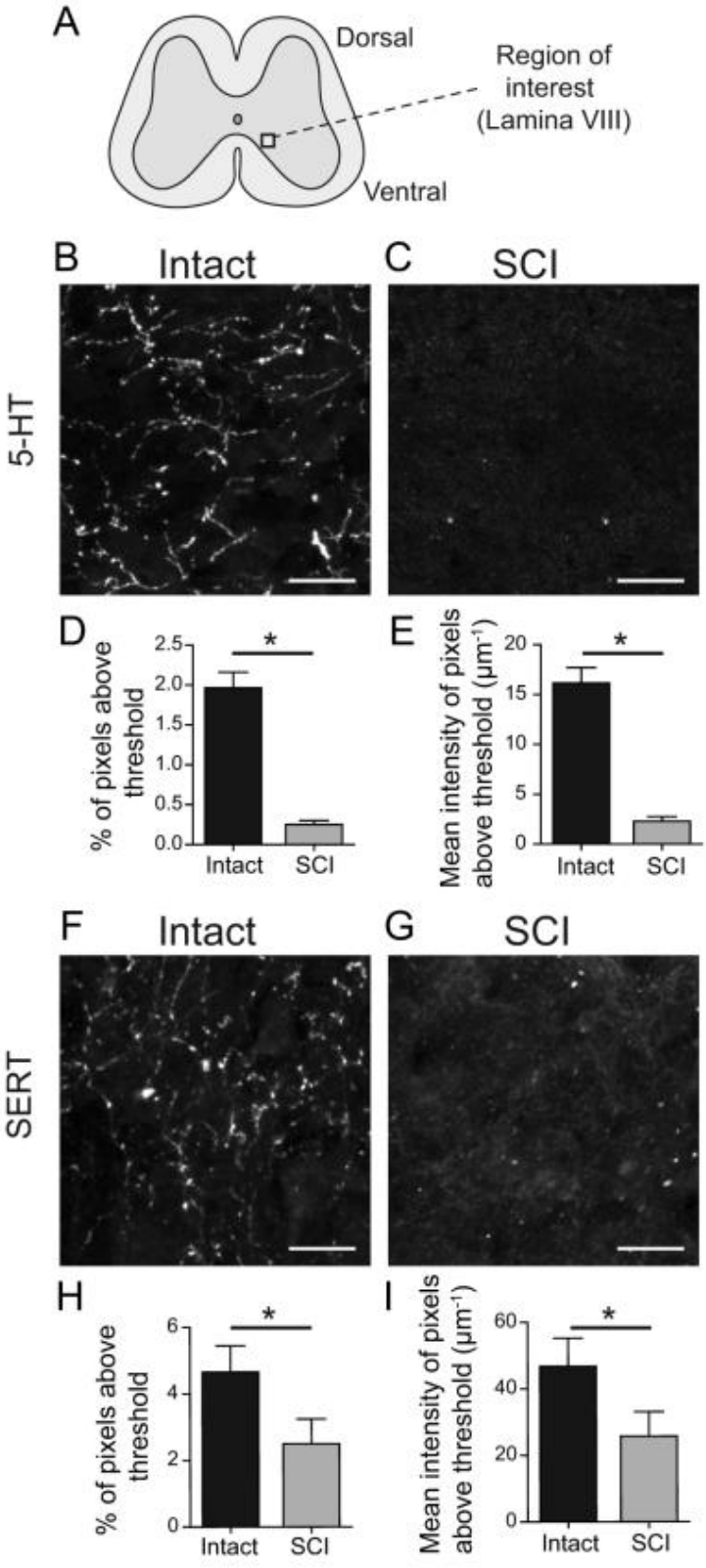

Figure 7. Reduction of serotonin (5-HT) and serotonin transporter (SERT) immunoreactivity after SCI. **A**. Spinal cord slice schematic with region of interest boxed around medial lamina VIII. **B, C**. 5-HT immunoreactivity from intact (**B**) and SCI (**C**) mice. **D, E**. Average area (**D**) and intensity (**E**) of 5-HT immunoreactivty in intact and SCI slices. **F, G**. SERT immunoreactivity from intact (**F**) and SCI (**G**) mice. H, I. Average area (**D**) and intensity (**E**) of SERT immunoreactivty in intact and SCI slices. *$p<0.05$, matched pair test, n=12 pairs for 5-HT and n=6 pairs for SERT. Scale bars: 10µm.

*The results listed under "Reduction in 5-HT and SERT after SCI" and Figure 7 were taken from Husch et al. (2012).

In order to test whether the remaining SERT labeling seen after SCI represented background non-specific labeling by the antibody or real expression of SERT in non-5-HT neurons, preabsorption controls were implemented. Preabsorption controls are used to verify the specificity of the SERT antibody to the mouse SERT peptide. In theory, all of the antibodies are inactivated since none are available to stain the SERT in the tissue with all of the antibodies binding to the peptide. Preabsorption of the SERT antibody with the SERT peptide epitope used to raise the antibody eliminated virtually all labeling in intact cords. In intact cords, while there was no difference between the preabsorption control and no-primary control, there was a significant difference between SERT labeling and the preabsorption control and between SERT labeling and no-primary control measures ($p<0.05$, One-way ANOVA, n=3, Figure 8). This illustrated that the SERT antibody is not showing a significant amount of non-specific binding to non-SERT antigens in intact spinal cord. In SCI cords, preliminary data using preabsorption of the SERT antibody with the SERT peptide epitope suggested that in SCI cords, the pre-absorbed antibody showed more immunofluorescence than the no-primary control. Empty black areas seen in Figure 9 are artifacts from the cryostat procedure and are not indicative of preabsorption control results. The difference between preabsorption of SERT antibody and no-primary control was not significant due to the low repetition number (n=3), but visual inspection suggested that the preabsorption control did show somewhat greater immunofluorescence than that of the no-primary control (Figure 9). This result can help begin to differentiate between real SERT expression after SCI and non-specific binding of the antibody. Although the SERT preabsorption control reduced SERT immunostaining in SCI cords, it did not reduce immunostaining to the level seen in the no-primary control; there was no statistically significant difference between

immunostaining of SERT in SCI cords and in the preabsorption control. This suggests that some of the staining observed in SCI cords may not be true SERT signals.

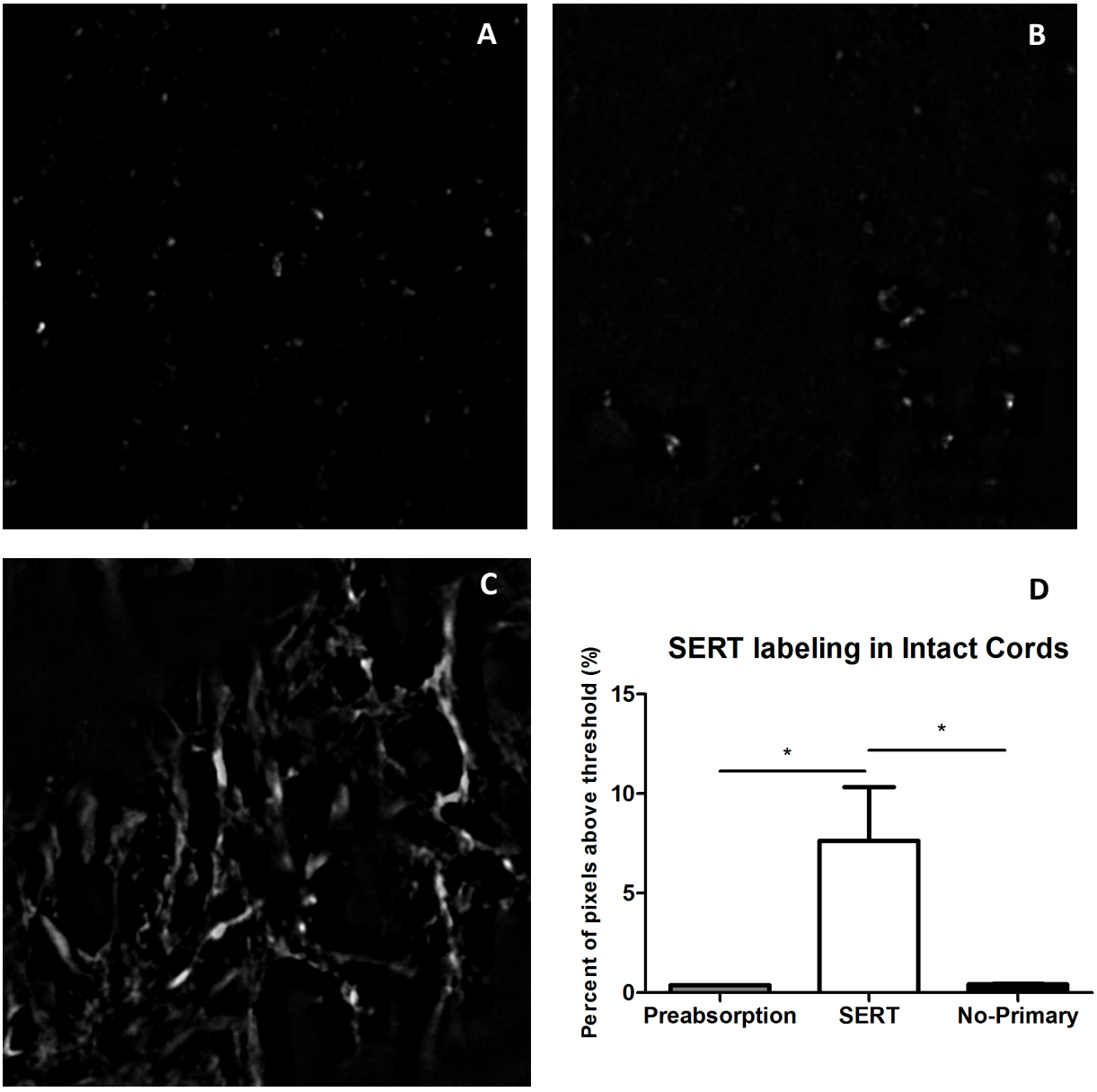

Figure 8. Immunohistochemistry controls for SERT labeling in intact cords. **A-C** were obtained from the same animal. **A**. No-primary control. **B**. Preabsorption control. **C**. SERT staining in intact cord. **D**. Average area of SERT staining in three different conditions. Asterisk denotes a statistically significant difference. Preabsorption of the SERT peptide with antibody effectively eliminated immunostaining comparable to that of the no-primary control condition.

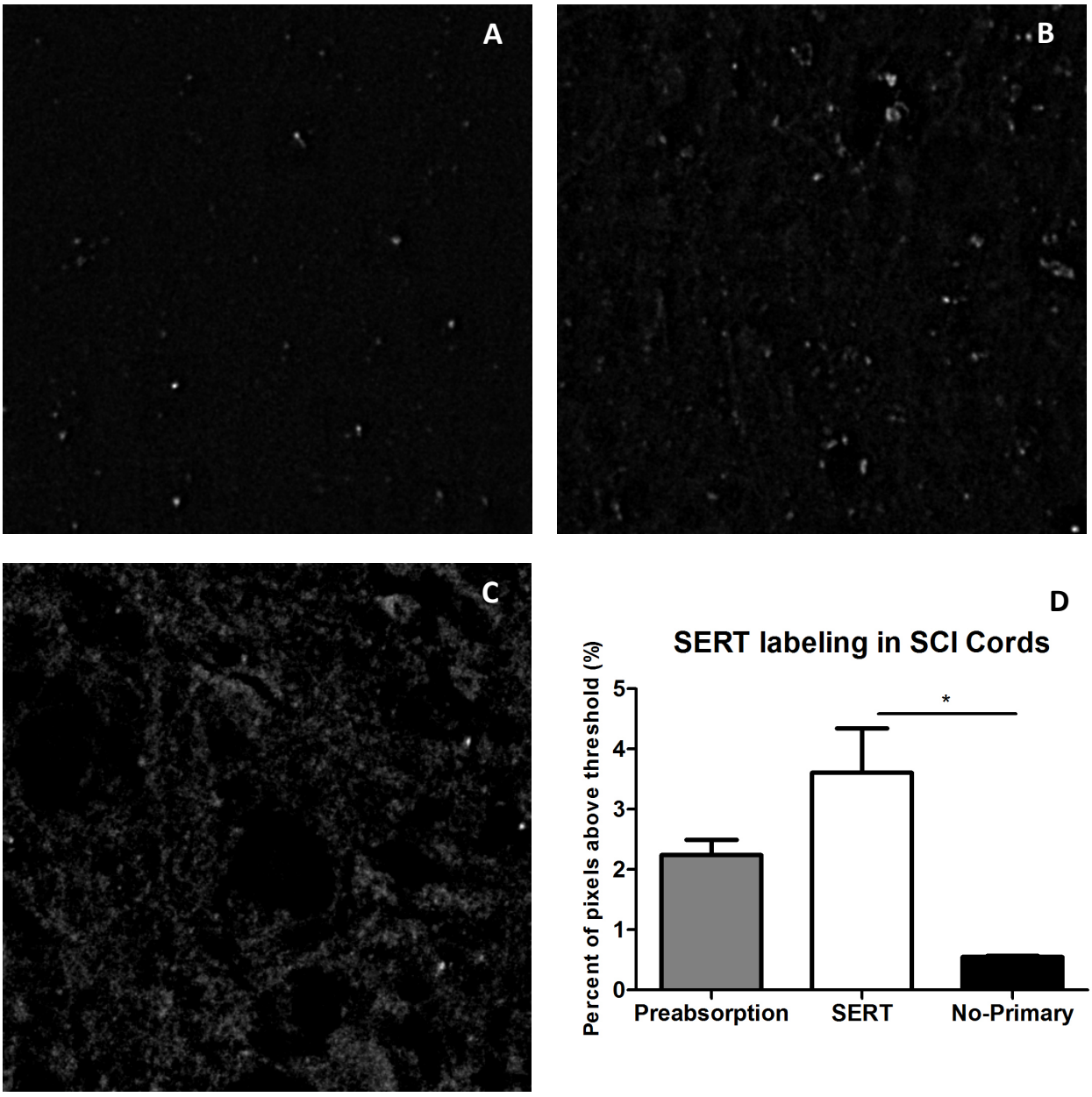

Figure 9. Immunohistochemistry controls for SERT labeling in SCI cords. **A-C** were obtained from the same animal. **A**. No-primary control. **B**. Preabsorption control. **C**. SERT staining in SCI cord. **D**. Average area of SERT staining in three different conditions. Asterisk denotes a statistically significant difference ($p<0.05$). While there was a decrease in SERT immunosignaling with the preabsorption, the difference between the immunosignaling of SERT in SCI cords and that of the preabsorption condition was not significant. Furthermore, the difference between preabsorption of SERT antibody and no-primary control was not significant, by visual inspection, the preabsorption control had greater immunofluorescence than that of the no-primary control.

Discussion

Spinal cord injury results in the loss of serotonergic fibers projecting from the brainstem to the spinal cord interneurons and motoneurons, and as a result, the concentration of 5-HT is significantly decreased in the spinal cord caudal to the lesion (Carlsson et al., 1963). In our single immunohistochemistry experiments, we expected to see significantly less 5-HT staining in SCI mice. Consistent with our hypothesis, four weeks after SCI, mice showed an 85% reduction in 5-HT expression as measured by pixel area, and an 84.6% reduction in 5-HT intensity in those pixels (Figure 7). Previous electrophysiological work has shown that V2a interneurons significantly increase their 5-HT sensitivity after SCI (Husch et al., 2012). In both intact and SCI cords, V2a interneurons were perfused with 5-HT, followed by a wash period to allow for a recovery to baseline parameters before a higher concentration of 5-HT was applied (Husch et al., 2012). V2a interneurons in intact cords did not significantly increase their firing rate with an application of 0.1 μM or 1 μM 5-HT, but 80% of these interneurons showed a significant increase in firing rate with an application of 10 μM 5-HT (Husch et al., 2012). In comparison, V2a interneurons in SCI cords significantly increased their firing rate with an application of as little as 10 nM 5-HT, reaching the maximal response at 0.1 μM 5-HT (Husch et al., 2012). With V2a interneurons in SCI cords showing a 100- to 1000- fold increase in 5-HT sensitivity, and with the fact that these interneurons are glutamatergic and excitatory to commissural interneurons and motoneurons, it is possible that greatly reduced presence of residual 5-HT in the spinal cord after SCI (Harvey PJ et al., 2006c) could account for this hypersensitivity (Husch et al., 2012). My double immunohistochemistry illustrating a clear co-localization of 5-HT with V2a processes (Figure 4), provides more evidence that V2a interneurons are directly innervated

by descending serotonergic fibers under control conditions. Thus, it is possible that loss of 5-HT is playing a major role in changing V2a interneuron properties.

From the double immunohistochemical staining of 5-HT with SERT in control spinal cords, I found that SERT strongly co-localizes with 5-HT axons, suggesting that most of the SERT is localized in serotonin terminals. Manders' coefficients illustrated that approximately 79% of the imaged SERT co-localized with the imaged 5-HT. This is a lower percentage than expected, since previous studies have shown that all the SERT is in 5-HT terminals. However, this may be explained by taking a closer look at the composite images (Figure 2C). Most of the red coloration from the SERT signal in the composite images surround the yellow pixels, or designated co-localized areas, and there are very few, if any, stand-alone red pixels. Furthermore, because Manders' coefficients are known to be very sensitive to background signal and local variations in intensity, these coefficients are most accurate when the intensities of the two channels are of similar value. Manders' coefficients thus illustrate when the intensity of one channel matches that of the second channel. This would suggest that SERT is primarily expressed in 5-HT processes, and the low M2 coefficient is more an artifact of the analysis threshold than a physical localization difference. The average M1 coefficient was 0.54, meaning approximately 54% of the imaged 5-HT co-localized with the imaged SERT. The fact that the M1 coefficient is less than the M2 coefficient illustrates that there is more 5-HT staining alone and not co-localizing with SERT. This may be because the areas of non-co-localization are the axonal pathways of 5-HT cells where SERT is not preferentially located, and the areas of co-localization are terminal fields where the synapses are located (Zhou et al., 1998).

Since I observed co-localization of SERT in 5-HT neuron processes (Figure 2), and similar co-localization patterns of SERT and V2a interneurons as 5-HT and V2a interneurons

(Figure 5 and 6), my finding of significantly reduced fibrous SERT immunostaining after SCI was expected. As with the 5-HT immunostaining, both the SERT area and the SERT intensity were significantly lower in SCI mice compared with intact mice. A 51.4% reduction in SERT area and a 49.4% reduction in SERT intensity were observed after SCI (Figure 7). This decrease in SERT immunoreactivity arises, in part, from the post-lesion degradation of serotonergic terminals as this is where SERT is primarily located (Zhou et al., 1998). Our results, differ from those of Hayashi et al. (2010), who observed a 99% loss of SERT in the ventral spinal cord after SCI in rats. However, this may be due to some of our SERT labeling actually being nonspecific background staining of the SERT antibody. Evidence for this explanation is seen from SERT antibody preabsorption control experiments. In theory, because all of the antibody should bind to the peptide containing the SERT epitope and thus inactivate the antibody in the tissue, preabsorption of the antibody with the SERT peptide should eliminate all SERT immunostaining. Thus, if the SERT labeling after SCI is all non-specific binding of the SERT antibody to other antigens, then I expect that the amount of SERT staining in the preabsorption control would be similar to that of the non-preabsorbed SCI slice labeling. In intact cords, there was a difference between SERT labeling and the preabsorption control and between SERT labeling and no-primary control measures, as expected if the SERT antibody is showing non-specific binding to non-SERT antigens (Figure 8). The critical test was then to compare the SERT labeling in SCI cords before and after preabsorption of the SERT antibody by the SERT-specific epitope. The preabsorbed SERT labeling in SCI cords was more similar to the SERT labeling from the SCI cords than in the intact cords, and higher than the no-primary controls (Figure 9). This may suggest that the observed SERT antibody labeling after SCI may not be from true SERT signals, but from non-specific binding that is not removed by preabsorption with

the SERT epitope. The non-specific background staining may be due to residual necrotic tissue in the spinal cord that is more prone to non-specific binding. However, the absence of non-specific staining using the 5-HT antibody argues against this hypothesis. Because my results seemed to show that there was more immunostaining in the SERT SCI cord than in the SCI preabsorbed control, both of which showed more immunostaining than the SCI no-primary control, this suggests that SERT may persist in non-5HT cells after SCI. However, these results are based on a low sample size (n=3), and more preabsorption control experiments must be performed in the future to make more conclusive observations.

Though SERT and 5-HT may be interacting within the same areas of the V2a interneurons, the loss of SERT may not be as much of a contributing factor to the SCI-induced CPG interneuron changes as the loss of serotonin. Previous electrophysiological experiments using citalopram, a SERT inhibitor, have shown that the loss of SERT on lesioned serotonergic terminals can only weakly account for the increase in 5-HT sensitivity (Husch et al., 2012). Applications of 0.1 μM, 1 μM, and 10 μM 5-HT to serotonin-sensitive control neurons treated with citalopram did not significantly increase firing rates (Husch et al., 2012). Because 5-HT sensitivity was not observed with the blockage of SERT, SERT loss is probably not a major contributing factor to 5-HT sensitivity.

With a complete sensory and motor function loss below the SCI site, axonal reconnections across the injury site and neural network maintenance below the injury site will be needed for a full recovery (Guertin, 2005). However, there is currently no treatment available for complete recovery from SCI since there are no such significant natural regenerative processes taking place in the spinal cord after SCI which would correct the changes in intrinsic properties of locomotor CPG neurons that occur due to the loss of 5-HT and other descending inputs

(Guertin, 2005). With further studies exploring the function of CPGs and of the changes SCI induces, we can work to discover methods of appropriately adjusting neural responses to SCI to help treat the more than 500,000 people suffering from spinal cord injury (Guertin, 2005).

Acknowledgements

This work was supported by NIH grants NS057599 and NS17323. I would like to thank Gabrielle Van Patten and Moira Scaperotti for their collaborative efforts with the single immunohistochemistry, Ben McLaughon for his technical assistance, Margaret Marchaterre for her help with the cryostat, Carol Bayles for her help with the confocal microscope, and the Cornell Statistical Consulting Unit for their help with statistical analysis. Finally, I would like to express my gratitude to Dr. Ronald Harris-Warrick and the rest of the lab group for their insights and continued support.

References

Barlow, SM. 2009. Central pattern generation involved in oral and respiratory control for feeding in the term infant. *Curr Opin Otolaryngol Head Neck Surg*. 17(3): 187–193.

Bennett DJ, Li Y, Siu M. 2001. Plateau potentials in sacrocaudal motoneurons of chronic spinal rats, recorded in vitro. *J Neurophysiol.* 86(4):1955-1971.

Carlsson A, Magnusson T, Rosengren E. 1963. 5-hydroxytryptamine of the spinal cord normally and after transection. Experientia. 19: 359.

Carlsson A, Falck B, Fuxe K, Hillarp NA. 1964. Cellular localization of monoamines in the spinal cord. Acta Physiol Scand. 60: 112-119.

Fourad K, Rank MM, Vavrek R, Murray KC, Sanelli L, Bennett DJ. 2010. Locomototion after spinal cord injury depends on constitutive activity in serotonin receptors. J Neurophysiol. 104: 2975-2984.

Guertin PA. 2005. Paraplegic mice are leading to new advances in spinal cord injury research. Spinal Cord. 43:459-461.

Harvey PJ, Li X, Li Y, Bennett DJ. (2006c). Endogenous monoamine receptor activation is essential for enabling persistent sodium currents and repetitive firing in rat spinal motoneurons. J Neurophysiol. 96: 1171-1186.

Hayashi Y, Jacob-Vadakot S, Dugan EA, McBride S, Olexa R, Simansky K, Murray M, Shumsky JS. 2010. 5-HT precursor loading, but not 5-HT receptor agonists, increases motor function after spinal cord contusion in adult rats. Exp Neurol. 221: 68-78.

Hughes DI, Bannister AP, Pawelzik H, Thomson AM. 2000. Double immunofluorescence, peroxidase labeling and ultrastructural analysis of interneurones following prolonged electrophysiological recordings in vitro. *Journal of Neuroscience Methods*. 101: 107-116.

Husch A, Van Patten GN, Hong DN, Scaperotti MM, Cramer N and Harris-Warrick RM. 2012. Spinal cord injury induces serotonin supersensitivity without increasing intrinsic excitability of mouse V2a interneurons. *J Neurosci*. 19 September 2012, 32(38):13145-13154.

Kong XY, Wienecke J, Chen M, Hultborn H, Zhang M. 2011. The time course of serotonin 2A receptor expression after spinal transection of rats: an Immunohistochemical study. *Neuroscience*. 177: 114 - 126.

Kiehn O. 2006. Locomotor circuits in the mammalian spinal cord. *Annu Rev Neurosci*. 29:279-306.

Kiehn, O. 2011. Development and functional organization of spinal locomotor circuits**.** Current Opinion of Neurobiology. 21(1):100-9

Langhammer CG, Previtera ML, Sweet ES, Sran SS, Chen M, Firestein BL. 2010. Automated Sholl Analysis of Digitized Neuronal Morphology at Multiple Scales: Whole Cell Sholl Analysis Versus Sholl Analysis of Arbor Subregions. *Cytometry Part A*. 77A: 1160-1168.

Manders EMM, Verbeek JF, Aten JA. 1993. Measurement of co-localization of objects in dual-color confocal images. Journal of Micorscopy. 169 (3): 375 – 382.

Nielsen K, Brask D, Knudsen GM, Aznar S. 2006. Immunodetection of the serotonin transporter protein is a more valid marker for serotonergic fibers than serotonin. *Synapse*. 59: 270-276.

Scaperotti, MM. 2012. Sublesional Changes to the Hindlimb Central Pattern Generator after Spinal Cord Injury in the Mouse: Investigating the Loss of Serotonin Transporter, and Dynamic 5-HT_{1A} Receptor Expression. 1-46.

Schmidt BJ, Jordan LM. 2000. The role of serotonin in reflex modulation and locomotor rhythm production in the mammalian spinal cord. Brain Res Bull 53(5):689-710.

Zhong G, Droho S, Crone SA, Dietz S, Kwan A, Webb WW, Sharma K, Harris-Warrick RM. 2010. Electrophysiological characterization of V2a interneurons and their locomotor-related activity in the neonatal mouse spinal cord. *J Neurosci* 30(1):170-182.

Zhou FC, Tao-Cheng J, Segu L, Patel T, Wang Y. 1998. Serotonin transporters are located on the axons beyond the synaptic junctions: anatomical and functional evidence. *Brain Res.* 805:241-254.